THE ASTROPHYSICAL JOURNAL, 517:L109–L112, 1999 June 1

GRB 990123: THE OPTICAL FLASH AND THE FIREBALL MODEL

RE'EM SARI[1] AND TSVI PIRAN[2]

Received 1999 February 2; accepted 1999 March 25; published 1999 April 8

ABSTRACT

We show that the ongoing observations of the remarkable burst GRB 990123 agree with the predictions of the fireball model. Specifically, the observations confirm the recent prediction that the reverse shock propagating into the ejecta would produce a very strong prompt optical flash. This reverse shock has also produced the 8.46 GHz radio signal, observed after 1 day. The forward shock, which is the origin of the classical afterglow, has produced the prompt X-ray signal as well as the late optical and IR emission. The observations suggest that the initial Lorentz factor of the ejecta was ~200. Within factors of order unity, this crude model explains all current observations of GRB 990123.

Subject headings: gamma rays: bursts — hydrodynamics — relativity — shock waves

1. INTRODUCTION

GRB 990123 triggered BATSE on 1999 January 23.507594 (Kippen et al. 1999). Using the Gamma-Ray Burst Coordinate Network (GCN;[3] Barthelmy et al. 1994), GRB 990123 triggered the Robotic Optical Transient Search Experiment (ROTSE), which discovered an 8.9 mag prompt optical flash (Akerlof et al. 1999). Such a strong optical flash was predicted, just a few weeks ago (Sari & Piran 1999a, 1999b; hereafter SP99a and SP99b, respectively), to arise from a reverse shock, propagating into the relativistic ejecta. Strong optical emission was also suggested earlier by Mészáros & Rees (1997) in two of several models they examined. SP99a and SP99b gave a lower limit of 15 mag for a "standard" γ-ray burst (GRB) with a fluence of 10^{-5} ergs cm^{-2}. Scaling that to the γ-ray fluence of GRB 990123 (3×10^{-4} ergs cm^{-2}) yields a lower limit of ~11 mag, compatible with the observed 9 mag.

The optical observations are depicted in Figure 1. The five last ROTSE exposures decay as a power law with a slope of ~ -2.0. We have inferred a slope of ~ -1.1 from the late *R*-band observations. A similar slope -1.13 ± 0.03 was deduced for the Gunn-*r* flux (Bloom et al. 1999; Yadigaroglu et al. 1999), significantly different from the initial slope. Several absorption lines show that the redshift of GRB 990123 is ≥ 1.61 (Kelson et al. 1999).

The GRB light curve has two clear, relatively hard, peaks with irregular softer emission that follow. *BeppoSAX*'s Wide-Field Camera (WFC) prompt X-ray light curve is complex, with only one clear peak (about 40 s after the main GRB peak). The peak flux of this burst is ~3.4 crab in the energy band 1.5–26 keV. An Narrow-Field Instrument (NFI) observation (Piro et al. 1999; Heise et al. 1999) started 6 hr after the burst depicts a power-law decay with a slope of -1.35 from the prompt observation (about 60 s after the burst) and within the 26 hr NFI observation.

A radio source at 8.46 GHz was detected on January 24.65 (Frail & Kulkarni 1999) with a flux density of 260 ± 32 μJy. Earlier and later observations revealed only 2 σ upper limits of 64 μJy (Frail & Kulkarni 1999; Kulkarni & Frail 1999). An earlier attempt to detect a radio source on 24.28 at 4.88 GHz gave only an upper limit of 130 μJy (Galama et al. 1999).

A detailed discussion of GRB 990123 observations is given in Kulkarni et al. (1999). We confront here the fireball theory with these observations. We show that the GRB light curve, the prompt optical flash light curve, the radio emission, as well as the available afterglow light curve for the first few days strongly support the reverse shock prompt emission model. This agreement provides additional support for the overall internal-external scenario.

2. AN OPTICAL FLASH FROM THE REVERSE SHOCK

The prompt optical and γ-ray emission are not correlated. The γ-ray counts ratios in the three optical exposures are 5 : 1 : 1 (examination of the spectrum shows that the energy ratio is about 10 : 1 : 1; D. Band 1999, private communication). The optical ratios are 1 : 15 : 5. Clearly, a strong optical signal from the cooling tail of the electrons producing the GRB itself would have been correlated with the γ-ray signal. Thus, the same electrons could not have emitted both the γ-rays and the optical emission. Moreover, GRB 990123 was a relatively hard burst peaking at about 1 MeV. The decreasing flux with decreasing frequency (below a few hundred keV) is incompatible with a low cooling frequency, which is required for a strong optical emission. We conclude that the γ-rays and the optical emission must have been emitted in different physical regions.

According to the fireball model (see, e.g., Piran 1999), shocks can take place in two possible regions: internal shocks within the relativistic ejecta and external shocks between the ejecta and the interstellar medium (ISM). The forward and reverse internal shocks are similar since they both run into ejecta shells with similar properties. On the other hand, the reverse external shock, which propagates into the dense ejecta, is very different from the forward external shock that propagates into the ISM. Therefore, overall there are three different emitting regions in the internal-external scenario.

The ratio between the typical synchrotron frequencies of the forward and of the reverse external shocks is proportional to γ^2, γ being the Lorentz factor of the ejecta (SP99a, SP99b). Thus, if an external reverse shock produces the GRB, the external forward-shock emission will be in GeV (Rees & Mészáros 1994). If an external forward shock has produced the GRB, the external reverse shock could have emitted in optical. However, such emission would have been correlated with the γ-ray emission. Thus, we rule out the external shock scenario,

[1] Theoretical Astrophysics 130-33, California Institute of Technology, Pasadena, CA 91125.
[2] Racah Institute of Physics, Hebrew University, Jerusalem 91904, Israel; Department of Physics, Columbia University, New York, NY.
[3] Available at http://gcn.gsfc.nasa.gov/gcn.

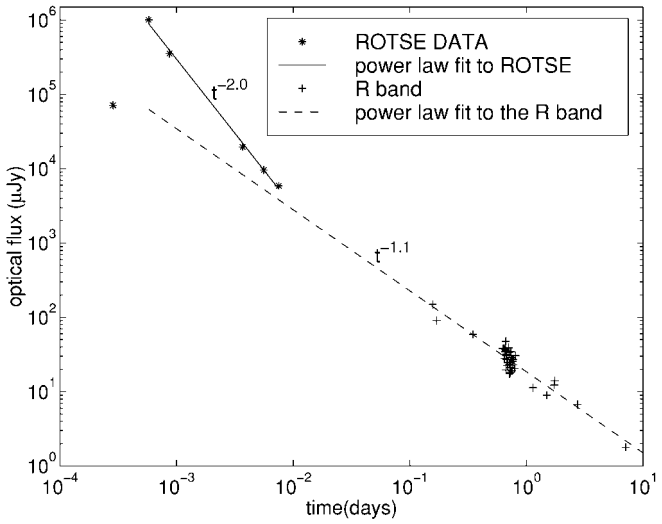

FIG. 1.—Optical light curve of GRB 990123. The early ROTSE measurements, excluding the first one, and the *R*-band data (Odewahn, Bloom, & Kulkarni 1999; Gal et al. 1999; Bloom et al. 1999; Zhu & Zhang 1999; Sokolov et al. 1999; Ofek & Leibowitz 1999; Masetti et al. 1999; Garnavich et al. 1999; Sagar et al. 1999; Yadigaroglu et al. 1999) are each described by a power law. The discrepancy between the two power laws is evident.

in agreement with other arguments against this model (Sari & Piran 1997; Fenimore, Madras, & Nayakshin 1996).

Within the internal-external scenario, the GRB is produced by the internal shocks. Here, the forward and reverse shocks are rather similar, emitting at the same energy band. If the forward external shock would have produced the prompt optical emission, there would have been no place to produce either the prompt X-rays or the late afterglow emission. Thus, the only possibility remaining is that the reverse external shock has produced the prompt optical emission while the forward external shock (which continued later as the afterglow) has produced the early X-ray as well as UV and some weak γ-ray signal. We will not expect any correlation between the γ-rays and the optical emission, but we expect some correlation between the optical emission and the early X-ray emission. Indeed, prompt X-ray emission peaked some 60 s after the beginning of the burst, not far from the peak exposure of ROTSE, and the overall γ-X spectrum shows a transition from hard to soft during the burst, suggesting a transition from one source of emission to another. The overlap between the internal shocks' signal (the GRB) and the early afterglow (the optical and the X-ray) was expected for a long burst such as GRB 990123. In this case, the internal shock emission would overlap the external shock emission (Sari 1997).

3. THE REVERSE-SHOCK EVOLUTION

A surprisingly good qualitative picture of the reverse-shock evolution can be obtained by treating the matter as a fluid, using the simplest assumptions (equipartition and random orientation) on the magnetic field evolution. The ejecta cools adiabatically after the reverse shock has passed through it. We assume that it follows the BM self-similar solution (Blandford & McKee 1976). (Strictly speaking, this solution deals only with the ISM material. Moreover, if the reverse shock is not very relativistic, the ejecta temperature quickly becomes nonrelativistic and would somewhat deviate from the BM solution.) In this solution, a given fluid element evolves with a bulk Lorentz factor of $\gamma \sim R^{-7/2}$. Since the observed time is given by $T \sim R/\gamma^2 c$, we obtain $\gamma \sim T^{-7/16}$. Similarly, the internal energy density evolves as $e \sim R^{-26/3} \sim T^{-13/12}$, the particle density evolves as $n \sim R^{-13/2} \sim T^{-13/16}$, and therefore the energy per particle, or the particle Lorentz factor, behaves like $\gamma_e \sim T^{-13/48}$.

To estimate the synchrotron emission, one needs to estimate the magnetic field and the electron distribution. The simplest assumption regarding the magnetic field is that its energy density remains a constant fraction of the internal energy density. In this case, we obtain $B \sim \sqrt{e} \sim T^{-13/24}$. Other evolutions of the magnetic field are possible if the magnetic field has a defined orientation (Granot, Piran, & Sari 1998a). The reverse shock has accelerated the electrons to a power-law distribution. Once the reverse shock crossed the ejecta, no new electrons are accelerated. All the electrons above a certain energy cool, and if the cooling frequency ν_c is above the typical frequency, we are left with a power-law electron distribution over a finite range of energies and Lorentz factors. Each electron now cools only because of the adiabatic expansion with its Lorentz factor proportional to $T^{-13/48}$.

Once the reverse shock has crossed the ejecta shell, the emission frequency of each electron drops quickly with time according to $\nu_e \sim \gamma\gamma_e^2 B \sim T^{-73/48}$. Given that the total number of radiating electrons N_e is fixed, the flux at this frequency falls like $F_{\nu_e} \sim N_e B\gamma \sim T^{-47/48}$. Below the typical emission frequency ν_m, we have the usual synchrotron low-energy tail so $F_\nu \sim F_{\nu_m}(\nu/\nu_m)^{1/3} \sim T^{-17/36}$. Above ν_m (and below ν_c), the flux falls sharply as $F_\nu \sim F_{\nu_m}(\nu/\nu_m)^{-(p-1)/2}$. For $p = 2.5$, this is about $F_\nu \sim T^{-2.1}$. Both ν_m and ν_c drop as $T^{-73/48}$, since all electrons cool by adiabatic expansion only. Once ν_c drops below the observed frequency, the flux drops exponentially with time.

Mészáros & Rees (1997) have derived different scaling laws for the reverse-shock emission. They used the same Lorentz factor and the same pressure for the ejecta and for the forward shock. However, as material accumulates between the ejecta and the forward shock, the ejecta lags behind the forward shock and it moves with a considerable lower Lorentz factor. It is also not in a pressure equilibrium with the forward shock.

4. COMPARISON WITH GRB 990123 OBSERVATIONS

The optical flux after the second ROTSE exposure decayed initially as T^{-2}, in agreement with the theory predicting -2.1. This means that ν_m, the typical synchrotron frequency of the reverse shock, is below the optical bands quite early on. Using the equation for the reverse-shock ν_m (SP99a, SP99b), we obtain

$$\nu_m = 1.2 \times 10^{14} \left(\frac{\epsilon_e}{0.1}\right)^2 \left(\frac{\epsilon_B}{0.1}\right)^{1/2} \left(\frac{\gamma_0}{300}\right)^2 n_1^{1/2} \le 5 \times 10^{14}. \quad (1)$$

This shows that the initial Lorentz factor of this burst was not too large. Using the equipartition values $\epsilon_e \sim 0.6$ and $\epsilon_B \sim 0.01$ and $n_1 = 5$ inferred for GRB 970508 (Wijers & Galama 1998; Granot, Piran, & Sari 1998), we find

$$\gamma_0 \sim 200. \quad (2)$$

The Lorentz factor at the beginning of the self-similar deceleration γ_A can be estimated from the time of the afterglow peak, ~50 s, to be $\gamma_A \sim 220$. Naturally, $\gamma_A \le \gamma_0$ (SP99a, SP99b). Since $\gamma_A \approx \gamma_0$, the reverse shock is only mildly relativistic and the initial Lorentz factor of its accelerated electrons' random motion is $\gamma_m \sim 630\epsilon_e$.

Emission from the reverse shock can also explain the radio

observations: a single detection of ~260 μJy 1 day after the burst. If the reverse-shock emission peaked in the optical at ~50 s and the peak frequency decayed in time as $T^{-73/48}$, then the peak frequency should have reached 8.4 GHz after ~19 hr. Scaling the observed optical flux of 1 Jy as $T^{-47/48}$ to 19 hr, the expected flux at $\nu_m = 8.4$ GHz is 840 μJy. From that time on, the 8.4 GHz flux decays as $T^{-2.1}$. The emitted 8.4 GHz flux is therefore given by

$$F_\nu = \begin{cases} 840\ \mu\mathrm{Jy}(T/19\ \mathrm{hr})^{-17/36}, & T < 19\ \mathrm{hr}, \\ 840\ \mu\mathrm{Jy}(T/19\ \mathrm{hr})^{-2.1}, & T > 19\ \mathrm{hr}, \end{cases} \quad (3)$$

so that at 1.2 days, when radio was detected, we expect a flux of 350 μJy, amazingly close to the observations. Equation (3) is also compatible with all later upper limits (see Fig. 2).

Equation (3) yields a 8.4 GHz flux of 1.5 mJy after 6 hr, which is way above the upper limit of 64 μJy. However, strong self-absorption of the reverse-shock radio emission takes place at this stage and suppresses this emission. When accounting for that, the resulting emission would be the minimum between the estimate of equation (3) (ignoring self-absorption) and the blackbody upper limit. This upper limit of blackbody emission from the reverse shock can be estimated by (Katz & Piran 1997; SP99b)

$$F_{\nu,\mathrm{BB}} = 2\pi\nu^2\gamma\gamma_e m_e \left(\frac{R_\perp}{D}\right)^2 = \begin{cases} 135\ \mu\mathrm{Jy}\ (T/19\ \mathrm{hr})^{5/12}, & T < 19\ \mathrm{hr}, \\ 135\ \mu\mathrm{Jy}\ (T/19\ \mathrm{hr})^{113/96}, & T > 19\ \mathrm{hr}. \end{cases} \quad (4)$$

Note that while the emission estimates uses only scaling with time of the observed early optical flux, the blackbody upper limit is more model dependent and possibly less reliable. The scaling in the last expression as well as the numerical coefficient use the scaling of γ and γ_e with time together with their initial values inferred from the initial afterglow time and flux. We used $R_\perp \sim 4.6\gamma cT$, where the numerical coefficient is appropriate for a quickly decelerating shell (Sari 1997, 1998; Waxman 1997a; Panaitescu & Mészáros 1998), and the relevant distance is $D = D_L/(1+z)^{1/2} \sim 1.7 \times 10^{28}$ cm for $\Omega = 1$, $h = 65$, and $z = 1.61$. At about 19 hr, ν_m drops below 8.4 GHz, causing an increase in the blackbody emission. Shown in Figure 2 is also this upper limit to the radio emission according to a blackbody spectrum. This upper limit from blackbody emission also accounts for the lack of 4.88 GHz emission reported by Galama et al. (1999).

We now turn to estimate the initial (50 s) cooling frequency ν_c. Initially, this frequency is the same for the forward and the reverse shocks (SP99a, SP99b). The temporal slope of the late afterglow (forward-shock) light curve and its spectrum, which are compatible with the predicted spectrum (Sari, Piran, & Narayan 1998) of slow cooling electrons indicate that the forward-shock cooling frequency is $\nu_{c,f}(2\ \mathrm{days}) \geq 4 \times 10^{14}$ Hz, leading to $\nu_c(50\ \mathrm{s}) = \nu_{c,r} = \nu_{c,f} \geq 2.5 \times 10^{16}$ Hz. A detection of a break in the optical flux later on would enable us to replace this inequality by a more solid number. A similar lower limit can be set using the fact that the reverse shock was seen for more than 650 s. The reverse-shock cooling frequency at that time is therefore higher than 5×10^{14} Hz. Scaling it back to 50 s according to $T^{-73/48}$, we get $\nu_c(50\ \mathrm{s}) \geq 2 \times 10^{16}$ Hz.

A more speculative constraint on ν_c can be obtained from the GRB spectrum itself (SP99a, SP99b). The decreasing GRB spectrum below a few hundred keV implies that $h\nu_c \geq 100$ keV. Otherwise, the low-energy flux would have increased at low frequencies like $\nu^{-1/2}$. This constraints $\nu_c \geq 2 \times 10^{19}$ Hz. This holds for the site producing the GRB (internal shocks). However, the observed γ-ray emission toward the end of the GRB is probably dominated by the forward shock, as suggested by the smoother temporal profile and by the softer spectrum. This means that a similar constraint applies to the initial ν_c of the forward shock, which is the same as the reverse shock one. If this rough estimate of 10^{19} Hz is correct, then the cooling break in the late optical light curve is not expected to be seen only after about 40 days.

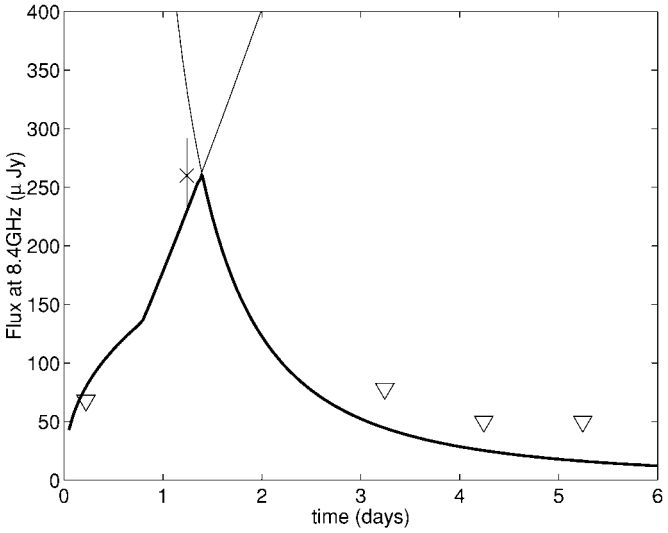

FIG. 2.—Single radio detection at 8.4 GHz (*crosses*) and the upper limits measured during the first five days (*triangles*). The decaying curve gives the emission from the reverse shock ignoring self-absorption. The rising curve gives the maximal flux allowed by self-absorption. The expected emission is the minimum between the two, shown as a heavy line.

The reverse-shock model can also be confronted with the observed optical–to–γ-ray energy ratio. Using the table in SP99b and the estimated synchrotron frequency at ~50 s ($\nu_m \sim 4 \times 10^{14}$ Hz) and the cooling frequency ($\nu_c \sim 10^{19}$ Hz), we expect the optical fluence to be 4×10^{-3} of the GRB fluence. This is about a factor of 5 higher than the observed ratio, a reasonable agreement considering the crudeness of the model. Note that this model assumes that the reverse shock contains the same amount of energy as the whole system. This can be of course lower by a factor of a few.

5. THE FORWARD SHOCK

The forward shock that propagates into the ISM is considered by now as the classical source of the afterglow (Katz 1994; Mészáros & Rees 1997; Vietri 1997; Wijers, Rees, & Mészáros 1997; Waxman 1997b; Katz & Piran 1997). After a possible short radiative phase, it becomes adiabatic and the shocked material acquires the BM profile. It then expands self-similarly until it becomes nonrelativistic. In GRB 990123, it has produced some of the prompt soft γ-rays and X-rays observed late during the burst by BATSE and the WFC. It has continued to produce the X-ray and the late optical and IR emission.

The initial decline of the X-ray suggests that already initially the typical synchrotron frequency was below the 1.5–10 keV band. The late slope of the light curve of the optical afterglow agrees well with other power-law decays seen in other afterglows. This suggests that we see an adiabatic decay phase. There could have been an early radiative phase, but if there was one it was shorter than the 3.75 hr gap before the first

optical observations. This is in agreement with expectations (Waxman 1997b; Granot et al. 1998a). The decline from 3.75 hr onward in the *R* band suggests that already at this stage the typical synchrotron frequency ν_m was below this band. Extrapolating this back to 50 s, we get $\nu_m \leq 2 \times 10^{18}$ Hz, consistent with the above discussion. Moreover, the ratio between ν_m of the forward and the reverse shock should be approximately γ^2. Using the two estimated values in the initial time, we find that $\gamma \sim 70$. This is a factor of 3 lower than the completely independent estimate in equation (2). Again, we consider this as a rather good agreement in view of the crudeness of both estimates. A short initial radiative phase could even improve this agreement.

The observed temporal decay slope of the X-ray (-1.35) and optical (-1.13) from the forward shock are comparable. An X-ray slope steeper by a quarter is predicted (Sari, Piran, & Narayan 1998) if the cooling frequency is between the X-rays and the optical. This prediction could be better tested with future data.

6. DISCUSSION

The discovery of prompt optical emission during a GRB has opened a new window to explore this remarkable phenomenon. The lack of correlation between the optical and γ-ray emission demonstrates that different processes produced the GRB and the optical emission. These findings are in perfect agreement with the internal-external model. Fenimore, Ramirez-Ruiz, & Wu (1999) reach the same conclusion on the grounds of the burst's temporal structure. Strong prompt optical emission was predicted (SP99a, SP99b) to arise from the reverse external shock. We see here that the overall fluence and the decay slope agree well with the predictions. The reverse shock also explains the origin of the transient radio observation a day after the burst and provide a crude measurement of the initial Lorentz factor $\gamma_0 \sim 200$.

The light curves of the X-ray and the late optical afterglow agree well with the, by now, "classical" afterglow model. According to this model, this emission is produced by the forward external shock. We expect a somewhat different slope for the X-ray and optical light curves. This can be tested with future data and analysis. We also expect that radio emission would show up on a timescale of weeks. The source of this emission would also be the forward external shock.

The late optical light curve (until submission of this Letter) is well fit by a single power law without any break. The index of this slope is approximately the one predicted by the spherical afterglow model. These facts suggest that so far there was no transition from spherical-like to expanding jet behavior. Such a transition is expected for a relativistic jet when the Lorentz factor reaches the value θ^{-1}, where θ is the opening angle of the jet (Rhoads 1997). Such a transition would lead to a break in the light curve and to a decrease in its index by more than 1. Since the theory gives a Lorentz factor of about 6 at 7 days, these observations set a lower limit on the beaming angle of GRB 990123 to be $\theta \geq 0.15$. The energy budget could still be "rescued" if a break is seen soon.[4]

This research was supported by the US-Israel BSF grant 95-328, by the Israeli Space Agency, by NASA grant NAG5-3516, and by the Sherman Fairchild Foundation. We thank E. Blackman, D. Band, and P. Kumar for helpful discussions.

[4] By now, such a break was discovered, implying $\theta_0 \sim 0.2$ (Kulkarni et. al. 1999).

REFERENCES

Akerlof, C., et al. 1999, GCN Circ. 205 (http://gcn.gsfc.nasa.gov/gcn/gcn3/205.gcn3)
Barthelmy, S. D., et al. 1994, in AIP Conf. Proc. 307, Second Huntsville Workshop, ed. G. Fishman, J. Brainerd, & K. Hurley (New York: AIP), 643
Blandford, R. D., & McKee, C. F. 1976, Phys. Fluids, 19, 1130
Bloom, J. S., et al. 1999, GCN 240 (http://gcn.gsfc.nasa.gov/gcn/gcn3/240.gcn3)
Fenimore, E. E., Madras, C., & Nayakshin, S. 1996, ApJ, 473, 998
Fenimore, E. E., Ramirez-Ruiz, E., & Wu, B. 1999, ApJ, submitted
Frail, D. A., & Kulkarni, S. R. 1999, GCN Circ. 211 (http://gcn.gsfc.nasa.gov/gcn/gcn3/211.gcn3)
Gal, R. R., Odewahn, S. C., Bloom, J. S., Kulkarni, S. R., & Frail, D. A. 1999, GCN Circ. 207 (http://gcn.gsfc.nasa.gov/gcn/gcn3/207.gcn3)
Galama, T. J., Vreeswijk, P., Rol, E., Strom, R., van Paradijs, J., Kouveliotou, C., & de Bruyn, G. 1999, GCN Circ. 212 (http://gcn.gsfc.nasa.gov/gcn/gcn3/212.gcn3)
Garnavich, P., Jha, S., Stanek, K., & Garcia, M. 1999, GCN Circ. 215 (http://gcn.gsfc.nasa.gov/gcn/gcn3/215.gcn3)
Granot, J., Piran, T., & Sari, R. 1998, preprint (astro-ph/9808007)
———. 1999, ApJ, submitted
Heise, J., DeLibero, C., Daniele, M. R., Scotti, G., Ricci, D., Capalbi, M., Antonelli, L. A., & Costa, E. 1999, IAU Circ. 7099
Katz, J. I. 1994, ApJ, 422, 248
Katz, J. I., & Piran, T. 1997, ApJ, 490, 772
Kelson, D. D., Illingworth, G. D., Franx, M., Magee, D., & van Dokkum, P. G. 1999, IAU Circ. 7096
Kippen, R. M., et al. 1999, GCN Circ. 224 (http://gcn.gsfc.nasa.gov/gcn/gcn3/224.gcn3)
Kulkarni, S. R., & Frail, D. A. 1999, GCN Circ. 239 (http://gcn.gsfc.nasa.gov/gcn/gcn3/239.gcn3)
Kulkarni, S. R., et al. 1999, Nature, 398, 391
Masetti, M., et al. 1999, GCN Circ. 233 (http://gcn.gsfc.nasa.gov/gcn/gcn3/233.gcn3)
Mészáros, P., & Rees, M. J. 1997, ApJ, 476, 232
Panaitescu, A., & Mészáros, P. 1998, ApJ, 492, 683
Odewahn, S. D., Bloom, J. S., & Kulkarni, S. R. 1999, IAU Circ. 7094
Ofek, E., & Leibowitz, E. 1999, GCN Circ. 210 (http://gcn.gsfc.nasa.gov/gcn/gcn3/210.gcn3)
Piran, T. 1999, Phys. Rep., in press (astro-ph/9810256)
Piro, L. 1999, GCN Circ. 203 (http://gcn.gsfc.nasa.gov/gcn/gcn3/203.gcn3)
Rees, M. J., & Mészáros, P. 1994, ApJ, 430, L93
Rhoads, J. E. 1997, ApJ, 487, L1
Sagar, R. 1999, GCN Circ. 227 (http://gcn.gsfc.nasa.gov/gcn/gcn3/227.gcn3)
Sari, R. 1997, ApJ, 489, L37
———. 1998, ApJ, 494, L49
Sari, R., & Piran, T. 1997, ApJ, 485, 270
———. 1999a, A&A, in press (astro-ph/9901105) (SP99a)
———. 1999b, ApJ, in press (astro-ph/9901338) (SP99b)
Sari, R., Piran, T., & Narayan, R. 1998, ApJ, 497, L17
Sokolov, V., Zharikov, S., Nicastro, L., Feroci, M., & Palazzi, E. 1999, GCN Circ. 209 (http://gcn.gsfc.nasa.gov/gcn/gcn3/209.gcn3)
Vietri, M. 1997, ApJ, 478, L9
Waxman, E. 1997a, ApJ, 491, L19
———. 1997b, ApJ, 485, L5
Wijers, R. A. M. J., & Galama, T. J. 1998, preprint (astro-ph/9805341)
Wijers, R. A. M. J., Rees, M. J., & Mészáros, P. 1997, MNRAS, 288, L51
Yadigaroglu, I. A., Halpern, J. P., Uglesich, R., & Kemp, J. 1999, GCN Circ. 242 (http://gcn.gsfc.nasa.gov/gcn/gcn3/242.gcn3)
Zhu, J., & Zhang, H. T. 1999, GCN Circ. 204 (http://gcn.gsfc.nasa.gov/gcn/gcn3/204.gcn3)